AD-A116 838 JOHNS HOPKINS UNIV LAUREL MD APPLIED PHYSICS LAB F/G 9/1
TECHNIQUES FOR DOPPLER SPECTRAL ESTIMATION OF HF RADAR SIGNALS --ETC(U)
JUN 82 R A GREENWALD N00024-78-C-5384
UNCLASSIFIED RADC-TR-82-67 NL

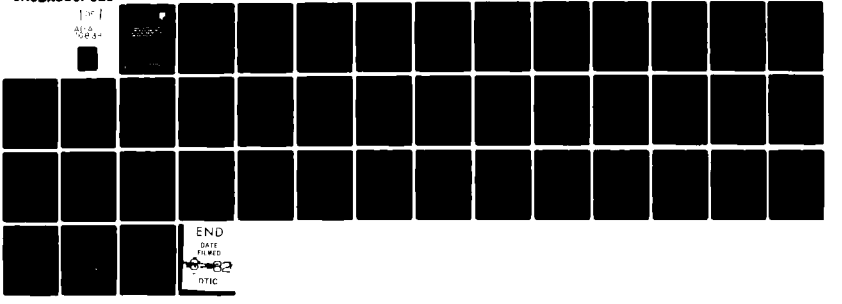

END
DATE FILMED
8-82
DTIC

(12)

RADC-TR-82-67
Final Technical Report
June 1982

TECHNIQUES FOR DOPPLER SPECTRAL ESTIMATION OF HF RADAR SIGNALS BACKSCATTERED FROM HIGH LATITUDE IONOSPHERIC IRREGULARITIES

The Johns Hopkins University

Greenwald, Raymond A.

ROME AIR DEVELOPMENT CENTER
Air Force Systems Command
Griffiss Air Force Base, NY 13441

This report has been reviewed by the RADC Public Affairs Office (PA) and is releasable to the National Technical Information Service (NTIS). At NTIS it will be releasable to the general public, including foreign nations.

RADC-TR-82-67 has been reviewed and is approved for publication.

APPROVED: William Ring

WILLIAM RING
Project Engineer

APPROVED: Allan C. Schell

ALLAN C. SCHELL
Chief, Electromagnetic Sciences Division

FOR THE COMMANDER: John P. Huss

JOHN P. HUSS
Acting Chief, Plans Office

If your address has changed or if you wish to be removed from the RADC mailing list, or if the addressee is no longer employed by your organization, please notify RADC (EEP) Hanscom AFB MA 01731. This will assist us in maintaining a current mailing list.

Do not return copies of this report unless contractual obligations or notices on a specific document requires that it be returned.

UNCLASSIFIED

SECURITY CLASSIFICATION OF THIS PAGE (When Data Entered)

REPORT DOCUMENTATION PAGE		READ INSTRUCTIONS BEFORE COMPLETING FORM
1. REPORT NUMBER RADC-TR-82-67	2. GOVT ACCESSION NO. AIIC-8378	3. RECIPIENT'S CATALOG NUMBER
4. TITLE (and Subtitle) TECHNIQUES FOR DOPPLER SPECTRAL ESTIMATION OF HF RADAR SIGNALS BACKSCATTERED FROM HIGH LATITUDE IONOSPHERIC IRREGULARITIES		5. TYPE OF REPORT & PERIOD COVERED Final Technical Report 1 Oct 80 - 30 Sep 81
		6. PERFORMING ORG. REPORT NUMBER N/A
7. AUTHOR(s) Raymond A. Greenwald		8. CONTRACT OR GRANT NUMBER(s) N00024-78-C-5384
9. PERFORMING ORGANIZATION NAME AND ADDRESS Applied Physics Laboratory/JHU Johns Hopkins Rd Laurel MD 20707		10. PROGRAM ELEMENT, PROJECT, TASK AREA & WORK UNIT NUMBERS 61102F 2305J230
11. CONTROLLING OFFICE NAME AND ADDRESS Deputy for Electronic Technology (RADC/EEP) Hanscom AFB MA 01731		12. REPORT DATE June 1982
		13. NUMBER OF PAGES 37
14. MONITORING AGENCY NAME & ADDRESS(if different from Controlling Office) Same		15. SECURITY CLASS. (of this report) UNCLASSIFIED
		15a. DECLASSIFICATION/DOWNGRADING SCHEDULE N/A

16. DISTRIBUTION STATEMENT (of this Report)

Approved for public release; distribution unlimited.

17. DISTRIBUTION STATEMENT (of the abstract entered in Block 20, if different from Report)

Same

18. SUPPLEMENTARY NOTES

RADC Project Engineer: William Ring (EEP)

19. KEY WORDS (Continue on reverse side if necessary and identify by block number)

Ionospheric irregularities	Doppler spectra
Ionospheric clutter	Cross spectral analysis
Over-the-horizon radars	Multipulse

20. ABSTRACT (Continue on reverse side if necessary and identify by block number)

This report examines various techniques for studying the Doppler spectrum of radar signals backscattered from high latitude ionospheric irregularities. Both pulsed and FM-CW techniques are considered and it is found that most approaches suffer from the need to have sufficiently high pulse or sweep repetition frequencies while at the same time avoiding range aliasing of the backscattered signals. Examples are presented of Doppler spectral observations with the various techniques. (Cont'd)

DD FORM 1 JAN 73 1473 EDITION OF 1 NOV 65 IS OBSOLETE

UNCLASSIFIED

SECURITY CLASSIFICATION OF THIS PAGE (When Data Entered)

This report also examines possible gains in discrete signal detection that may result from cross spectral analysis of backscattered radar signals. Studies presented in this report indicate that, while there is improvement in detection, it is not as large as has been previously expected.

TABLE OF CONTENTS

1.0 INTRODUCTION

Recently, increased interest has been directed toward obtaining better understanding of the nature of electron density irregularities in the F-region of the high latitude ionosphere. Two areas of particular interest are the mechanisms by which these irregularities are created and the Doppler spectral characteristics that these irregularities introduce when scattering radiowaves in the HF (3-30 MHz) frequency band. It is felt that these characteristics may be useful in understanding the mechanisms that produce the irregularities. Also, knowledge of the Doppler spectral characteristics is essential for assessing the clutter effects that these radars might have on HF radar systems.

During the past year, several Doppler spectral studies have been conducted using the Air Force bistatic research radar at Ava and Verona, New York; a French scientific radar at Lycksele, Sweden; and the NSF/NOAA HF sounder at Fairbanks, Alaska. All of these facilities utilize different Doppler spectral detection schemes, and each have advantages and disadvantages. In this report we describe the different techniques and results from each of these facilities. We also describe a new instrument utilizing a multipulse technique that should become operational within a few months. The multipulse techniques will be implemented on a radar operating in a selectable fixed frequency pulse mode; however, it may equally well be implemented on a swept-frequency radar such as the Ava-Verona facility through some modification of that system.

During the past year an appreciable effort was also devoted toward evaluating a new technique for decreasing the detrimental effects that broadbanded clutter spectra have on HF radar systems. The elements of this technique are described in the 1980 Final Report entitled Doppler Spectral Characteristics of High Latitude Ionospheric Irregularities (Greenwald, 1980). Results of this effort are described in this report.

2.0 DOPPLER TECHNIQUES USED IN STUDYING HIGH LATITUDE F-REGION IRREGULARITIES

In this report we consider four different techniques for studying the spatial and temporal dependence of Doppler-spectral characteristics associated with HF radar backscatter from high latitude F-region irregularities. The techniques are:

1) FM-CW
2) repetitive pulse
3) variable-lag double pulse
4) multiple pulse

The FM-CW technique is the method presently used by the Ava-Verona bistatic radar. It utilizes repetitive synchronized linear frequency sweeps (quadratic phase variation) in both the transmitter and receiver. If the transmitter and receiver sweep together, then a signal transmitted at frequency F and scattered from range R_0 would return to the receiver when it is tuned to a central frequency of $F_0 + 2BR_0/C'$. Here B is the sweep rate of the transmitter and receiver in units of megahertz per second and C' is the average group velocity of the radio frequency signal along the path. The frequency offset associated with the distance to the scattering element is independent of the instantaneous operating frequency; thus the demodulated signal at the output of the receiver has a frequency spectrum determined by the relative strength of the backscattered signal as a function of range.

With the FM-CW method one uses Fourier analysis to obtain the scattered signal level as a function of range. A detail description of this process and the ambiguity function associated with it is given in Rihaczek (1969). For the purpose of this report it is sufficient to note that the complex Fourier coefficients for each frequency band are nearly equivalent to the range dependent quadrature outputs of a phase coherent receiver in a pulsed radar. The single difference is that scatterers moving with appreciable velocity are Doppler shifted to appear as if they were located at a different range.

The analogy between repetitively swept FM-CW radars and repetitively pulsed fixed frequency radars may be carried one step further. Let us assume that there is a stationary scatterer such as a mountain at range R_0. Then at a group delay $\tau = 2R_0/C'$, the quadrature outputs of a phase coherent receiver would maintain constant values. In a like manner, if the mountain were to scatter a signal from an FM-CW radar, then the complex Fourier coefficient corresponding to the frequency $2BR_0/C'$ and range R_0 would also remain constant with time. Alternatively, if the scatterer at range R_0 were moving, then both the quadrature receiver outputs at group delay τ and the complex Fourier coefficient at frequency $2BR_0/C'$ would be changing with time and they would change in an identical manner.

We can now consider a series of consecutive pulses from a fixed frequency radar or consecutive sweeps of an FM-CW radar. From these one can obtain a series of consecutive samples of the output of the phase coherent receiver at group delay τ or a series of consecutive values for the complex Fourier coefficient corresponding to frequency $2BR_0/C'$. Either of these series may be taken as a time series which may be Fourier transformed to yield the Doppler spectrum of the scatterers located at range R_0.

When performing Doppler spectral analysis, certain restrictions must be taken into account. Firstly, the Doppler width and mean Doppler velocity of the scatterers at range R_0 determine the repetition frequency of the FM-CW sweeps and the fixed frequency radar pulses. Ideally these should be in excess of twice the maximum frequency in the scatterer's Doppler spectrum for a given radar wavelength. For example, if the scatterers possess velocities of 1000 m/s relative to a radar operating at 15 MHz, then the repetition frequency should be in excess of 200 Hz.

Having selected a repetition frequency for the radar pulse or sweep rate, one is immediately confronted with the second restriction. With high repetition frequencies, it is entirely possible that the receiver will receive backscatter from multiple ranges simultaneously. For a fixed frequency radar with a repetitive frequency of 200 Hz, scatterers at a group delay τ would be superimposed upon scatterers at group delays of τ+ 5 ms, τ + 10 ms, etc. In a like manner for a FM-CW system, scatterers located at R_0/C' would be

superimposed upon scatterers at $R_0/C' + 5$ ms, etc. The severity of this problem is ultimately dependent on three parameters: 1) the radar operating frequency, 2) the radial velocity distribution of the scatterers, and 3) the range interval over which backscatter is observed.

As we have described Doppler spectral studies using repetitively pulsed radars along with our description of FM-CW radars, there is no need to describe this approach further. It should, however, be noted that the French SAFARI radar located in Lycksele, Sweden operates in a repetitively pulsed selectable fixed-frequency mode.

The variable lag double-pulse technique is an approach in which one may obtain unaliased measurements of large Doppler velocities while simultaneously avoiding the problem of superimposing backscatter from a number of different ranges. This approach involves the determination of the complex autocorrelation function rather than the Doppler spectrum. However, once the autocorrelation function is obtained the Doppler spectrum may be determined by Fourier transformation.

We can understand the double pulse approach as follows: consider two pulses emitted by a transmitter and separated by time t. They are scattered from a target at range R_0. At time delay τ after each pulse a backscattered response will appear at the receiver. Initially, let us assume the target to be discrete and moving toward or away from the radar with constant velocity. The sampled outputs of the quadrature receiver may be denoted as:

$$C_1(\tau) = A_1(\tau) + iB_1(\tau) \qquad 2.1$$

$$C_2(\tau,t) = A_2(\tau,t) + iB_2(\tau,t) \qquad 2.2$$

where the subscripts 1 and 2 denote the sample associated with the first and second transmitter pulse at group delay τ. The autocorrelation function $R(\tau,t)$ is given by

$$R(\tau,t) = C_1^*(\tau)C_2(\tau,t) \qquad 2.3$$

It possesses real and imaginary parts given by

$$X(\tau,t) = A_1(\tau)A_2(\tau,t) + B_1(\tau)B_2(\tau,t) = \alpha \cos(2vt/\lambda) \qquad 2.4$$

and

$$Y(\tau,t) = A_2(\tau)B_1(\tau,t) - A_1(\tau)B_2(\tau,t) = \alpha \sin(2vt/\lambda) \qquad 2.5$$

where α is a constant, v is the radial velocity of the target and λ is the wavelength corresponding to the radar operating frequency. One can see that the real and imaginary parts of the autocorrelation function trace out sinusoids that are in quadrature. If these quantities are determined at discrete lag increments, $t=nt_0$, between the two transmitted pulses, then the resulting values could be Fourier transformed to yield a line spectrum at $f = \pm 2v/\lambda$. The sign of the Doppler shift is determined by whether the target is moving toward or away from the radar.

In the case of a distributed target or one moving with variable velocity the analysis is slightly more complex. The problem is described in greater detail by Rummler (1968). For the present report it is sufficient to note that the autocorrelation functions will generally appear as damped sinusoidal functions.

We can now consider some of the advantages of the variable-lag double pulse. Since we have only transmitted a double pulse rather than a repetitive string of pulses, at any time the receiver will receive the backscattered return from no more than two ranges. Moreover, in the cross product calculation only one range will contribute to an average non-zero result. This can be seen by allowing 2.1-2.2 to be generalized so that there are targets at different ranges. Then

$$C_1 = A_1(\tau_1) + iB_1(\tau_1) + A_2(\tau_0) + iB_2(\tau_0) \qquad 2.6$$

$$C_2 = A_1(\tau_2,t) + iB_1(\tau_2,t) + A_2(\tau_1,t) + iB_2(\tau_1,t) \qquad 2.7$$

where the quadrature receiver output C_1 contains backscattered contributions from the first transmitted pulse at group delay τ_1 and from the second transmitted pulse at group delay $\tau_0 < \tau_1$, and C_2 contains contributions from the first transmitted pulse at group delay $\tau_2 > \tau_1$ and from the second transmitted pulse at group delay τ_1. Under the generally valid assumption that backscatter from distinct ranges is statistically independent, one can see that

$$\langle R(\tau_1,t)\rangle = \langle C_1 C_2^*\rangle \qquad 2.8$$

$$= \langle [A_1(\tau_1) + iB_1(\tau_1)]\ [A_2(\tau_1,t) + iB_2(\tau_1,t)]\rangle$$

where $\langle\ \rangle$ denotes the expectation value. Note that this result is essentially independent of the spacing between the two transmitted pulses. Hence, very large Doppler velocities may be correctly analyzed without superimposing contributions from distinct ranges. In this operational mode one must only take care that the spacing between double pulse pairs is sufficiently large so backscatter is received from only one pulse pair at a time.

In terms of comparison it is possible to consider the equivalent autocorrelation function that results from a repetitive transmitter pulse sequence. One can, for example, rewrite (2.6-2.7) as

$$C_1 = A_0(\tau_2) + iB_0(\tau_2) + A_1(\tau_1) + iB_1(\tau_1) + A_2(\tau_0) + iB_2(\tau_0) \qquad 2.9$$

$$C_2 = A_1(\tau_2,t) + iB_1(\tau_2,t) + A_2(\tau_1,t) + iB_2(\tau_1,t) + A_3(\tau_0,t) + iB_3(\tau_0,t)$$

where subscripts 0-3 on the A's and B's denote four sequential pulses in a repetitive pulse series. The associated autocorrelation function is given by

$$\langle R(\tau,t)\rangle = \langle C_1 C_2^*\rangle \qquad 2.10$$

$$= \langle [A_0(\tau_2) + iB_0(\tau_2)]\ [A_1(\tau_2,t) + iB_1(\tau_2,t)]\rangle$$

$$+ \langle [A_1(\tau_1) + iB_1(\tau_1)]\ [A_2(\tau_1,t) + iB_2(\tau_1,t)]\rangle$$

$$+ \langle [A_2(\tau_0) + iB_2(\tau_0)]\ [A_3(\tau_0,t) + iB_3(\tau_0,t)]\rangle .$$

Thus, by using repetitive pulse we have superimposed the results from three distinct group delays, τ_2, τ_1, and τ_0 .

In fairness it should be noted that the variable lag double pulse is rather inefficient in terms of maintaining a high average power output. This is especially true for the longer lags of the autocorrelation function for which the transmitter is generally inactive. The approach also assumes that the scattering process is time stationary during the interval that the various lags of the autocorrelation function are being calculated. Often and especially in the high latitude ionosphere this is not the case.

The variable lag double pulse approach has been used for spectral measurements with the STARE radar system in Scandanavia and with the NSF/NOAA HF sounder at Fairbanks, Alaska. With the latter instrument difficulties due to the non-stationarity of the scattering process were readily apparent.

A vast improvement over the simple variable lag double pulse scheme is the multipulse approach. In this technique one transmits a number of pulses with carefully selected spacings. The criteria for choosing the pulse pattern are: 1) that one should obtain with one pulse burst as many lags of

an autocorrelation function as possible and 2) that one should avoid pulse schemes that allow superposition of different group delays. Farley (1972) has presented a number of possible schemes for incoherent scatter measurements. For HF measurements in the high latitude ionosphere the problem is somewhat less restrictive, and it is possible to choose pulse schemes that Farley may not have considered. In particular, the pulse scheme shown in Figure 2.1 is one that is presently being implemented on a HF radar for high latitude irregularity studies.

The pulse pattern shown in Figure 2.1 utilizes seven transmitted pulse with spacings of $2t_0$, t_0, $4t_0$, $6t_0$, $2t_0$ and t_0. This combination contains all possible lags for zero to $16t_0$. If one examines the possible lags from this sequence one sees that there are two possible group delays that will contribute to lags of t_0, $2t_0$ and $3t_0$. However, these group delays are separated by $10t_0$. Assuming a minimum value of t_0 = 2ms, one sees that the range ambiguity occurs only if there is concurrent scatter from regions with group delays differing by at least 20 ms. This is an extremely unlikely event even for HF backscatter and thus it may be safely ignored. There also is a range ambiguity for a lag of $13t_0$ with three distinct group delays contributing to the cross product. However, as there should be relatively little residual correlation remaining at this long lag, the potential confusion may, with caution, be ignored.

With the multipulse technique there is a considerable increase in average transmitted power. If we consider a sixteen lag autocorrelation function then the time required to transmit a complete 16 lag multipulse pattern is $16t_0$. In contrast, if one uses variable lag double pulse methods, the complete transmission would require $128t_0$. In addition, for a multipulse pattern one needs to allow for the group delay to the scattering region only once, whereas for the double pulse approach one must include this group delay for each lag of the correlation function. Thus the multipulse approach is at least eight times as efficient as the variable lag double pulse approach and its efficiency increases approximately linearly with the number of lags in the correlation function.

A shortcoming of the multipulse approach is that there is increased noise due to uncorrelated scatter from unwanted ranges (e.g. contribution such as those in Equation 2.6-2.7). Fortunately for HF studies, the entire transmitted pulse generally does not cause concurrent backscatter at the receiver and, therefore, the problem is considerably less severe that it might appear.

There is one final and <u>important</u> point with respect to the spectral and correlation techniques described in this section. Specifically, it is entirely possible to combine the FM or quadratic phase techniques with the double pulse or multiple pulse techniques. Under these circumstances a pulse would be replaced with a linear FM sweep with duration less than t_0. Also, control must be included to determine the occurrence and spacing of the FM sweeps. One would then calculate a Fourier transform for each sweep to obtain the complex Fourier coefficients corresponding to each group delay and use these coefficients in (2.8) in the same manner as one would use the quadrature outputs of a phase coherent receiver. This combination would produce a rather efficient transmission made with relatively high averge power and no range ambiguities or Doppler spectral aliasing.

3.0 DOPPLER SPECTRA FROM HIGH LATITUDE F-REGION IRREGULARITIES

Having considered a variety of methods for the determination of Doppler spectra and autocorrelation functions from high latitude F-region irregularities, we now examine some typical results. Figures 3.1-3.6 represent examples of Doppler spectra observed with the Ava-Verona FM-CW system during the evening hours. The measurements were made on 27 January 1981 between 0100-0300 UT (2000-2200 local time). For these measurements the radar was swept over the frequency range 16.387-16.389 MHz with a sweep rate of 100 KHz/s and the receiving antenna was directed toward geographic north (approximately 10° to the west of geomagnetic north). The times given represent universal time. The range index represents the range interval for which the Doppler spectrum is analyzed. For these examples the range is determined by multiplying the index value by 75 km. In the case of Figure 3 the range corresponds to 1350 km.

Given the operational parameters, the Doppler spectra in Figures 3.1-3.6 have an aliasing frequency of 25 Hz which corresponds to a radial velocity of approximately 230 m/s. Ignoring for the moment the narrow spectral peak at +25 Hz (this will be discussed in the next section), one sees that the Doppler spectra are generally quite broad. The narrowest Doppler width is observed in Figure 3.2 where it is aproximately 160 m/s and the widest is observed in Figure 3.6 where the spectrum is virtually flat. Clearly, most of the spectra are rather strongly frequency aliased and have spectra widths in excess of 250 m/s.

One can attempt to locate the peak of each of the spectra; however, again due to the frequency aliasing, the values may not be correct even with regard to the sign of the shift. This is due to the fact that spectral aliasing beyond the Nyquist frequency comes in at the negative Nyquist frequency as can be seen in Figure 3.5. Thus the evidence in the data of sign changes in the mean Doppler shift is quite possibly due to changes in the magnitude of a unidirectional drift velocity.

In an attempt to obtain unaliased spectra an experiment was conducted on 10 April 1981 with a sweep repetition frequency of 200 Hz and an

average operating frequency of 18.5 MHz. For this study a Doppler velocity of 810 m/s would have produced frequency aliasing. Unfortunately, the resulting Doppler spectra were quite similar to Figure 3.1, which again suggested frequency aliasing. No further tests were conducted at these high sweep repetition frequencies.

It is worthwhile comparing these Doppler observations with some theoretical expectations as to the motions of F-region irregularities. Greenwald (1980) has postulated that F-region irregularities might drift under the influence of the ionospheric electric field. In this case, the drift at these local times would be westward with a magnitude of a few hundred to more than one thousand meters per second. As the radar is directed to the west of geomagnetic north, a negative Doppler shift is expected. In the figures positive Doppler shifts are at times observed. While this may indicate an inconsistency with the electric field drift hypothesis, it is also possible that it is indicative of spectral aliasing. Clearly, better spectral results are required.

The French-Swedish SAFARI radar (Hanuise et al., 1981) has now been operating for one year. In this period, a number of campaigns have been conducted and results similar to those shown in Figure 3.7 have been obtained. In this example, the radar was operated in the 14 MHz amateur band with a 5° horizontal beamwidth directed toward geographic north (~ 12° to the east of corrected geomagnetic north). The radar was operated in a pulse mode with a pulse repetition frequency of 100 Hz.

One can see in Figure 3.7 that with a pulse repetition frequency of 100 Hz there was relatively little frequency aliasing of the spectra. The spectral widths varied from 8-24 Hz (80-250 m/s) and the mean Doppler shifts ranged from 200-380 m/s. At the local time of this measurement (~ 2315) the electric field induced drift would be in a southwestward direction. The sign of the Doppler shift is consistent with this expected drift; however, with only a single Doppler component it is difficult to estimate what the total irregularity drift speed is. It should be noted that there are range dependent variations in the observed Doppler velocity which may be associated with spatial variation of magnitude and/or direction of an electric field induced drift.

4.0 ELIMINATION OF SPREAD SPECTRA

In a recent report Greenwald (1980) suggested that cross spectral analysis might be used to eliminate spread Doppler spectra associated with ionospheric irregularities while retaining discrete spectra that might be associated with aircraft. The essence of this approach was to calculate the time-averaged cross spectrum of two lagged data sets for which the lag time was greater than the decorrelation time of the ionospheric process contributing to the broad spectral component.

Using Equations 5.9 - 5.16 from Greenwald (1980) we can write

$$S'(R,\omega) = A(\omega)\ B^*(\omega) \qquad 4.1$$

as the cross spectrum of the signal that is backscattered from range R. One may express the complex Fourier coefficients $A(\omega)$ and $B^*(\omega)$ in terms of discretely sampled time series. These are given by

$$A(R,n,\mu) = \frac{1}{N} \sum_{J=0}^{N-1} X(R,j,\mu)W(j)\exp(-2\pi ijn/N) \qquad 4.2$$

$$B(R,n,\mu) = \frac{1}{N} \sum_{J=0}^{N-1} X(j+C,\mu)W(j)\exp(-2\pi ijn/N) \qquad 4.3$$

where $X(R,j,\mu)$ is the complex demodulated output of the receiver at the group delay corresponding to range R, $W(j)$ is the data window (Blackman and Tukey, 1959), and μ is the number of the data set when multiple data sets are being transformed. Assuming N samples per data set and a sampling frequency f_s, each data set is obtained in the time

$$\Delta T = N/f_s \qquad 4.4$$

while the lag time between the data sets used in the cross spectral determination is

$$T = C/f_s \qquad 4.5$$

The cross spectral estimator is then given by

$$P_{xx_c}(n) = \sum_{\mu=1}^{M} A(n,\mu)B^*(n,\mu) \qquad 4.6$$

and the variance of this estimator is

$$\sigma(n,M) \tilde{\sim} S(R,n)/\sqrt{M} \qquad 4.7$$

where M is the number of spectra that are averaged and S(R,n) is the spectral power in frequency interval n of the signal backscattered from range R. It has a spectral estimator given by

$$P_{xx}(n) = \sum_{\mu=1}^{M} A(n,\mu)A^*(n,\mu) \qquad 4.8$$

If the lag time T is sufficiently large that A(n, μ) and B(n,μ) are uncorrelated, then for M $\rightarrow \infty$, the cross spectrum will average to zero incoherently. That is

$$P_{xx_c}(n) \approx P_{xx}(n)/\sqrt{M} \tilde{\sim} \sigma(n,M) \qquad 4.9$$

In contrast contributions to A(n,μ) and B(n,μ) that remain coherent after lag time T will maintain the same power level in the cross spectrum as in the power spectrum.

While the results to be presented in this section support these conclusions, they also bring out a point that had been overlooked in the previous report (Greenwald, 1980). Specifically, these results show that ones ability to discern a discrete target within a spread spectrum is controlled by the variance of the spectral estimators. Since the variance of both the power spectrum and cross spectrum decrease at a rate that is approximated by (4.7),

one method does not have any significant advantage over the other. In practice, the cross spectral approach does appear to have a variance that is 3 dB less than the power spectral approach. This difference may be due to the fact that both the in-phase and quadrature portions of the cross-spectrum are being averaged in cross-spectral calculation.

During the past year, several studies have been conducted to evaluate the usefulness of the cross spectral approach. The narrow spectral peak located at the right hand edge of the Doppler spectra in Figures 3.1 - 3.6 represent an additional discrete frequency inserted into the receiver to simulate the presence of a discrete target. These figures represent the average of 100, 200 and 400 Doppler power spectra and one sees that, aside from the added signal, the variance in the spectral estimates is typically of the order of that which one would expect.

The same data have been used to calculate the cross spectral power within the Doppler spectra for a lag time of 1.28 s. That is, instead of calculating the Doppler power spectrum, two sets of Fourier coefficients obtained 1.28 s apart were cross multiplied to yield the Doppler cross power spectrum. The results are shown in Figures 4.1-4.6. In these examples, one can see the reduction of the overall level of the Doppler spectrum. In Figures 4.1 and 4.6 it is roughly 10% of the levels in Figure 3.1 and 3.6. In Figures 4.2-4.4 for which 200 spectra were averaged, the level is approximately 7% of the level in Figures 3.2-3.4. Finally in Figure 4.5 for which 400 spectra were averaged, the level of the background spectrum is only 5% of that in Figure 3.5 (note the change in the vertical axis scaling for Figure 4.5).

If one compares the discrete, inserted frequency in Figures 3.1-3.6 and 4.1-4.6, one sees that there is no measureable reduction in this component as a result of cross spectral analysis. Any reduction in the frequency band containing the inserted frequency is a reduction in the ionospheric signal on which the inserted frequency is sitting.

Again, comparing Figure 3.1-3.6 and 4.1-4.6, one sees that in all cases the discrete spectrum is easier to identify in the latter spectra than in the former. Also, the variance of the spectral estimators of the cross

spectra appears to be less than those of the power spectra as has been noted previously. However, in all cases for which the discrete frequency is readily identifiable in the cross spectrum, I believe it could also be identified in the power spectrum albeit with greater difficulty.

In passing it should be noted that cross spectral analysis may also be used for the first Fourier transform of the FM-CW technique. When used for this purpose it is also capable of discerning discrete targets. Figure 4.7 illustrates the range dependence of the backscattered signal on Day 346 at 0344 UT. In this example, each 100 Hz corresponds to a range interval of 150 km with zero Hertz having been offset to a range of 1200 km and the spectra have been plotted on a log scale. The spectral peaks observed at integral multiples of 50 Hz represents a modulation of the backscattered signal by the sweep repetition frequency of the transmitter.

The cross power spectrum shown in Figure 4.8 utilizes the same data as has been used to obtain Figure 4.7; however, the spectra have been calculated with a 1 second lag. Here one sees that the signal level is approximately 15 dB less than that in Figure 4.7 commensurate with the nearly 1000 spectra that have been averaged to obtain these results.

One final point should be made with regard to both power or cross spectral analyses. If a transmitter has a pulse or sweep repetition frequency of 64 Hz and one is calculating 64 sample Doppler spectra, then one second is required to obtain the data for one spectrum. In order to average 100 spectra, 100 seconds of data is required. Due to a number of reasons such as changing ionospheric conditions, 100 seconds is probably the practical upper limit for averaging spectra. The variance of the spectral estimators when 100 spectra are averaged is 10% implying that it is unlikely that one could identify a discrete signal that is more than 10 dB below the total Doppler power in any given frequency band.

5.0 SUMMARY

In this report we have considered several techniques used in FM-CW and pulsed radars for obtaining the Doppler sectrum associated with high latitude F-region electron density irregularities as observed at HF frequencies. It is found that one is typically confronted with the conflicting problems of pulsing or sweeping the radar at a sufficiently high repetition frequency to avoid frequency aliasing of the Doppler spectrum while at the same time avoiding range aliasing of the backscattered signals. Results obtained with the FM-CW radar at Ava-Verona, New York and a French-Swedish radar at Lycksele, Sweden indicate that mean Doppler velocities and Doppler widths in excess of 400 ms may not be uncommon. For radars operating in the frequency range of 15-20 MHz, this would require repetition frequencies of at least 100 Hz. With these repetition frequencies the unambiguous range resolution is 10 ms or 1500 km. While there are periods for which such conditions may be satisfied, at other times higher repetition frequencies may be required or the backscatter may be extended over greater ranges. Under these circumstances more sophisticated pulse modulation techniques should be sought.

One approach which might be used to a greater degree is the multipulse technique. This technique utilizes special pulse or FM sweep patterns that enable one to determine most or all of the lags of an autocorrelation function. Having obtained the autocorrelation function one can easily determine the Doppler spectrum via Fourier transformation. The multipulse approach is particularly powerful since it allows one to obtain very high equivalent pulse or sweep repetition frequencies while avoiding ambiguity as to the range of the backscattered signal.

In this report we also present the results of several tests on determining the usefulness of cross spectral analysis as a means of separating discrete and spread spectra. While the results show that cross spectral analysis enables easier identification of discrete spectral contributions within a spread background spectrum, considerable improvements are not be be expected. This conclusion is reached by noting that the standard deviation of the spectral estimators in the cross spectrum is only slightly less than the

standard deviation of power spectral estimators. Furthermore, the ratio of these standard deviations is independent of the number of power or cross spectra that have been averaged. Since ones ability to discern a discrete spectral contribution is ultimately limited by the intensity of this component with respect to the standard deviation of the spectral estimators, only nominal improvements can be expected.

ACKNOWLEDGEMENTS

The author would like to thank Dr. J.-P. Villain of L.S.E.E.T., University of Toulon, France, for providing examples of the data obtained with the French-Swedish radar at Lycksele, Sweden.

REFERENCES

Blackman, R. B. and T. W. Tukey, The Measurement of Power Spectra (Dover, New York) 1959.

Farley, D. T., Multiple-pulse incoherent scatter correlation function measurements, Radio Sci., 7, 661, 1972.

Greenwald, R. A., Doppler spectral characteristics of high latitude ionospheric irregularities: Effect on HF radars, 1980 Final Report, RADC/EEP, 1980.

Hanuise, C., J.-P. Villain and M. Crochet, F-region plasma instabilities in the auroral zone observed with a coherent HF radar system, Geophys. Res. Letter, In Press, 1981.

Rihaczek, A. W., Principles of High-Resolution Radar (McGraw-Hill, New York) 1969.

Rummler, W. D., Two pulse spectral measurements, Tech. Memo, MM-68-4121-15, Bell Telephone Laboratories, Whippany, NJ, 1968.

FIGURE CAPTIONS

FIGURE 2.1 Seven transmitter pulse pattern that provides autocorrelation function lags from 0-16 t_0. This pattern has range ambiguity for lag 13 t_0. At HF frequencies there will, in general, not be any range ambiguity for lags t_0, 2 t_0, and 3 t_0.

FIGURE 3.1 Doppler spectrum of F-region irregularities at a range of 1350 km at 0105 UT on 27 January 1981 (Ava-Verona radar).

FIGURE 3.2 Doppler spectrum of F-region irregularities at a range of 1350 km at 0111 UT on 27 January 1981 (Ava-Verona radar).

FIGURE 3.3 Doppler spectrum of F-region irregularities at a range of 1350 km at 0118 UT on 27 January 1981 (Ava-Verona radar).

FIGURE 3.4 Doppler spectrum of F-region irregularities at a range of 1350 km at 0129 UT on 27 January 1981 (Ava-Verona radar).

FIGURE 3.5 Doppler spectrum of F-region irregularities at a range of 1350 km at 0132 UT on 27 January 1981 (Ava-Verona radar).

FIGURE 3.6 Doppler spectrum of F-region irregularities at a range of 1125 km at 0230 UT on 27 January 1981 (Ava-Verona radar).

FIGURE 3.7 Range dependent Doppler spectra (group delay 5.6-8.6 ms) of F-region ionospheric irregularities as observed with the French-Swedish radar at Lycksele, Sweden.

FIGURE 4.1 Doppler cross spectrum obtained from the data used in Figure 3.1. Discrete frequency inserted at 25 Hz.

FIGURE 4.2 Doppler cross pectrum obtained from the data used in Figure 3.2. Discrete frequency inserted at 25 Hz.

FIGURE 4.3 Doppler cross spectrum obtained from the data used in Figure 3.3. Distrete frequency inserted at 25 Hz.

FIGURE 4.4 Doppler cross spectrum obtained from the data used in Figure 3.4. Discrete frequency inserted at 25 Hz.

FIGURE 4.5 Doppler cross spectrum obtained from the data used in Figure 3.5. Discrete frequency inserted at 25 Hz.

FIGURE 4.6 Doppler cross spectrum obtained from the data used in Figure 4.6. Discrete frequency inserted at 25 Hz. Note change of gain on ordinate axis.

FIGURE 4.7 Range Fourier transform of FM-CW receiver output from the Ava-Verona radar on 11 December 1980. Spectral lines are due to modulation of the received signal by the repetition frequency of the FM-CW sweep.

FIGURE 4.8 Same range Fourier transform as in Figure 4.7 except the power profile is calculated using cross spectral analysis with a 1 second lag. Note the overall 15 dB reduction in the signal level due to lack of coherence over this lag time.

7-PULSE PATTERN FOR 16-LAG AUTOCORRELATION FUNCTION

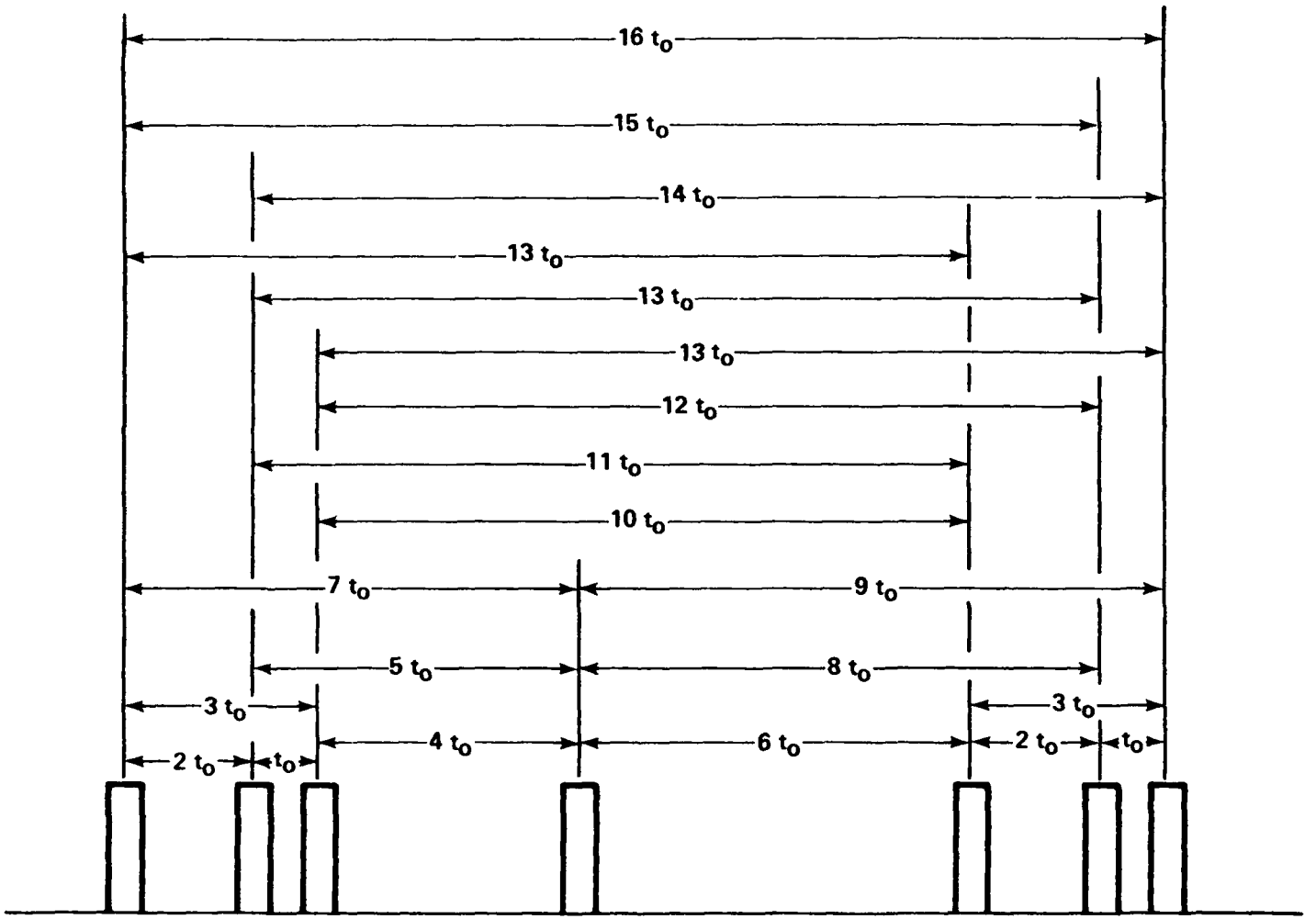

FIGURE 2.1

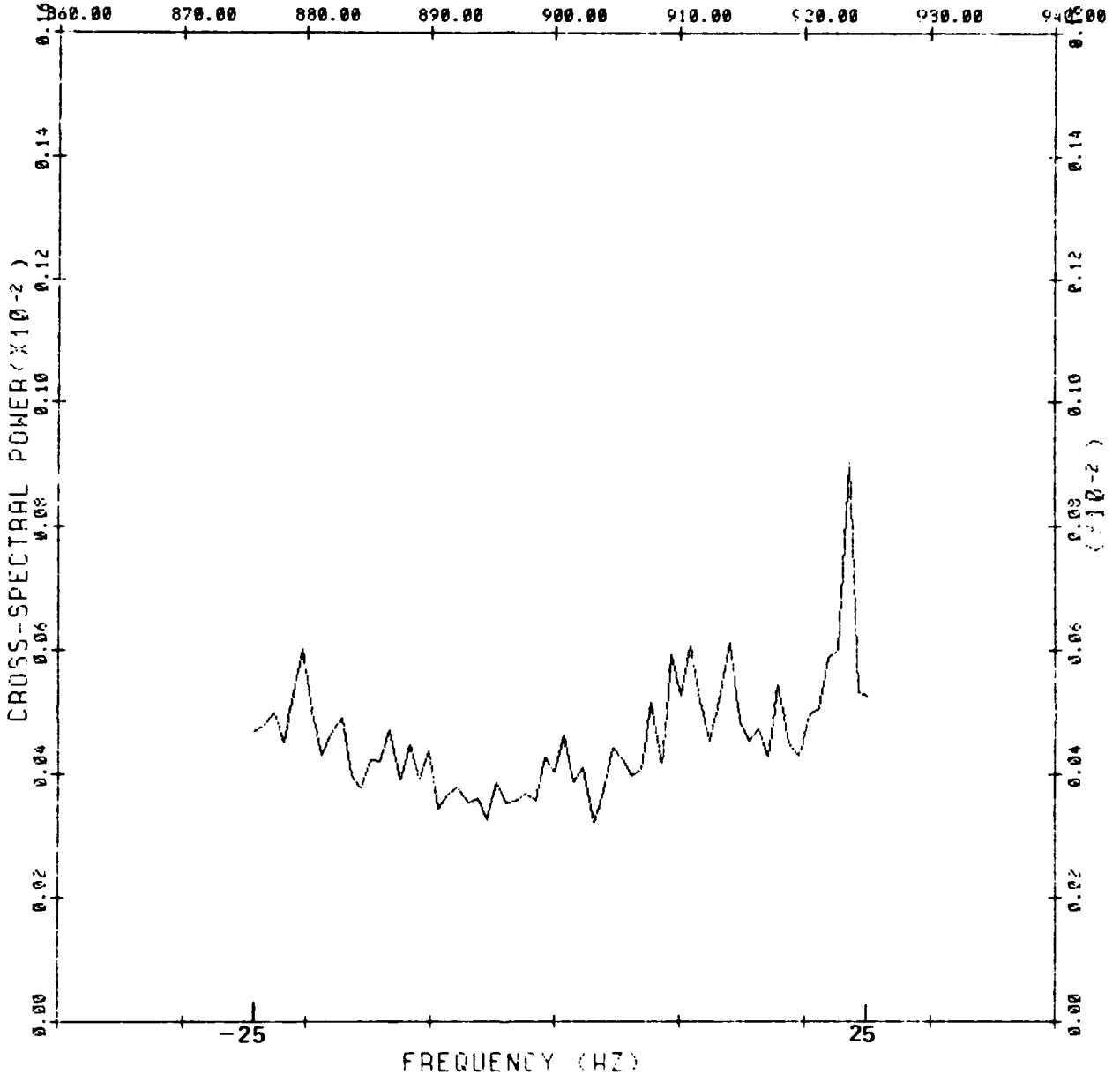

DAY: 27 HOUR: 1 MIN.: 5 SEC.: 30
LAG IN SECONDS FOR CROSS SPECTRUM: 0.00
NUMBER OF SPECTRA AVERAGED: 100
RANGE INDEX: 18

FIGURE 3.1

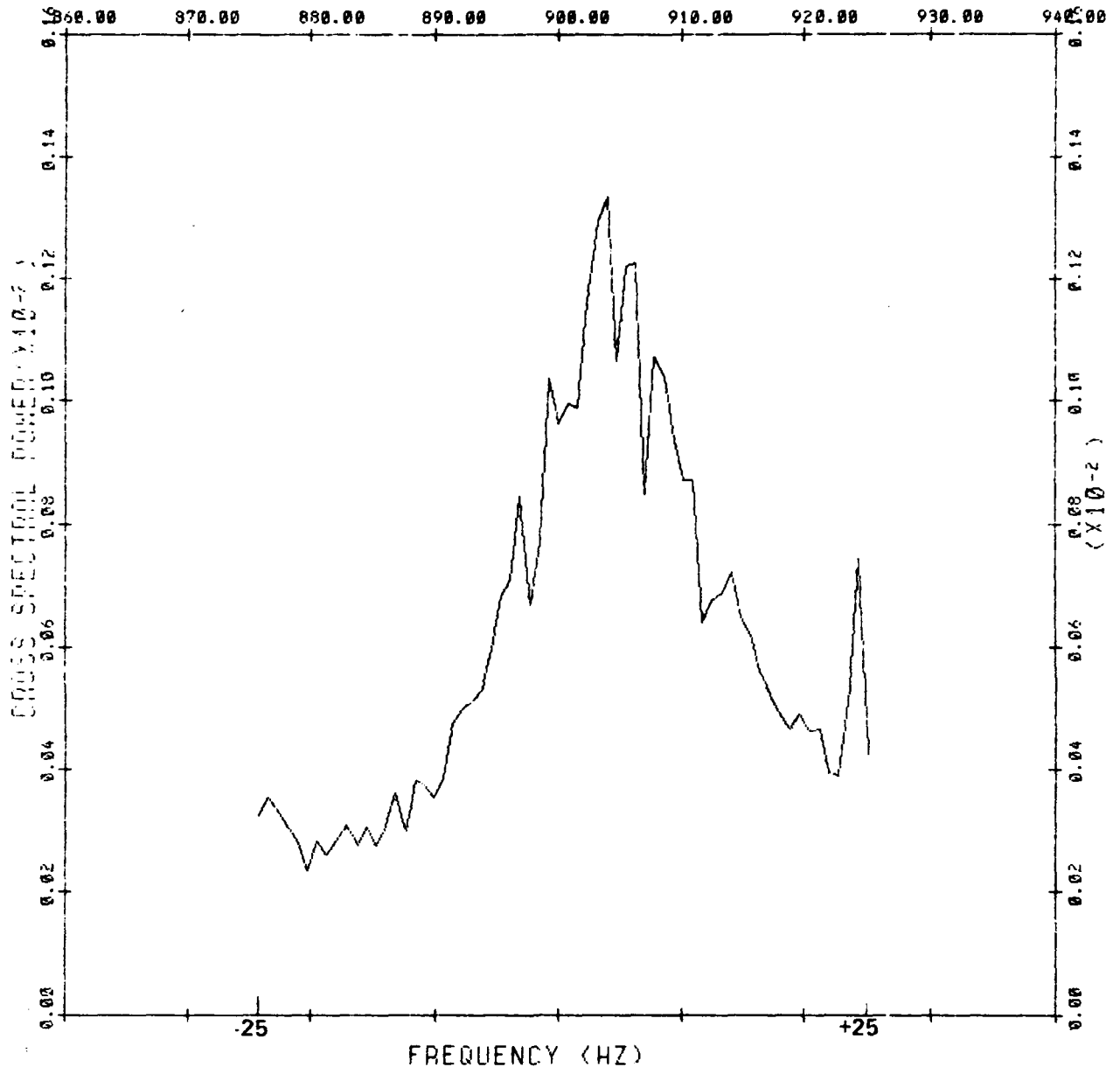

DAY: 27 HOUR: 1 MIN.: 11 SEC.: 0
LAG IN SECONDS FOR CROSS SPECTRUM: 0.00
NUMBER OF SPECTRA AVERAGED: 200
RANGE INDEX: 18

FIGURE 3.2

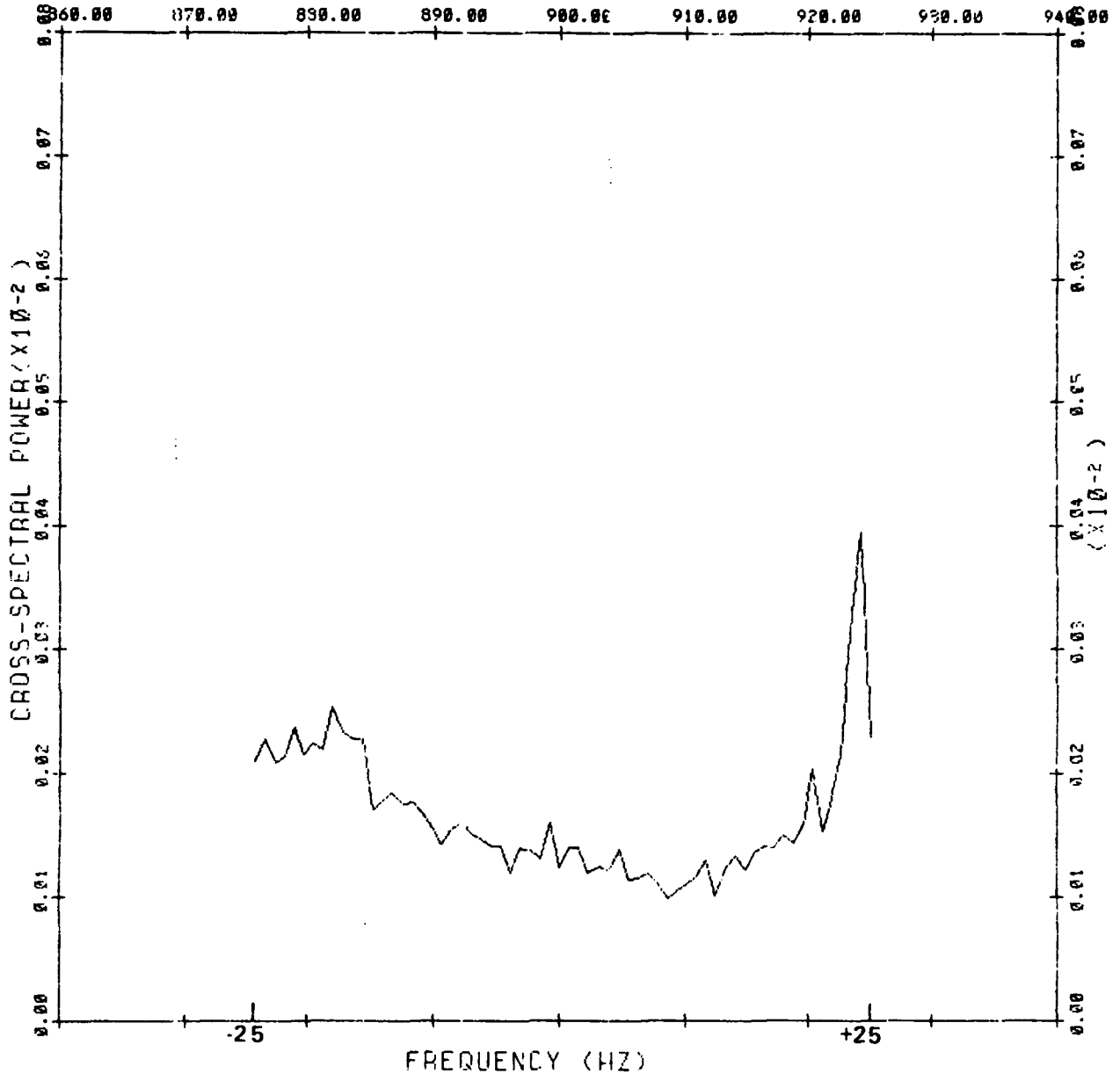

DAY: 27 HOUR: 1 MIN.: 18 SEC.: 0
LAG IN SECONDS FOR CROSS SPECTRUM: 0.00
NUMBER OF SPECTRA AVERAGED: 200
RANGE INDEX: 18

FIGURE 3.3

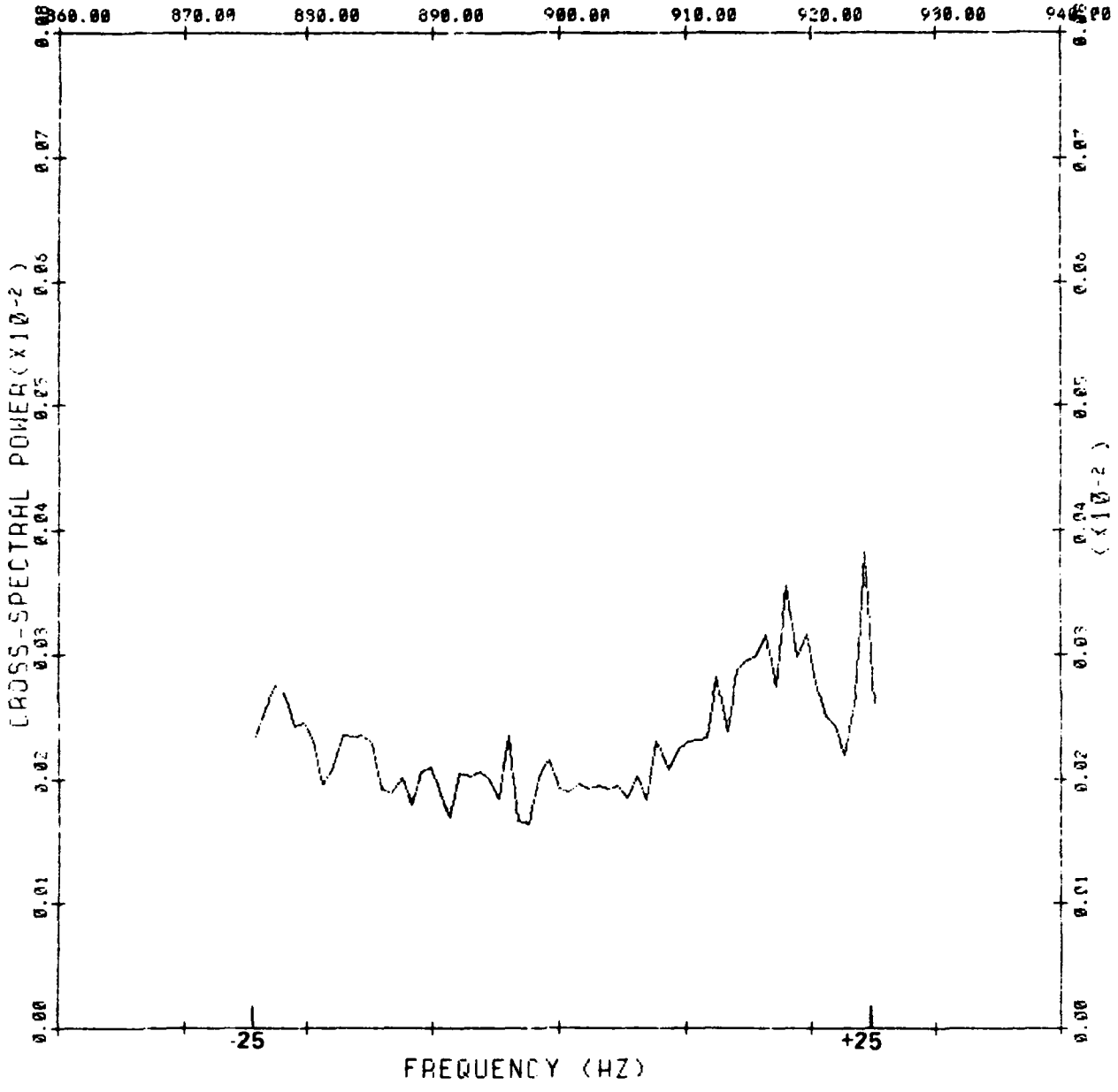

DAY: 27 HOUR: 1 MIN.: 29 SEC.: 0
LAG IN SECONDS FOR CROSS SPECTRUM: 0.00
NUMBER OF SPECTRA AVERAGED: 200
RANGE INDEX: 18

FIGURE 3.4

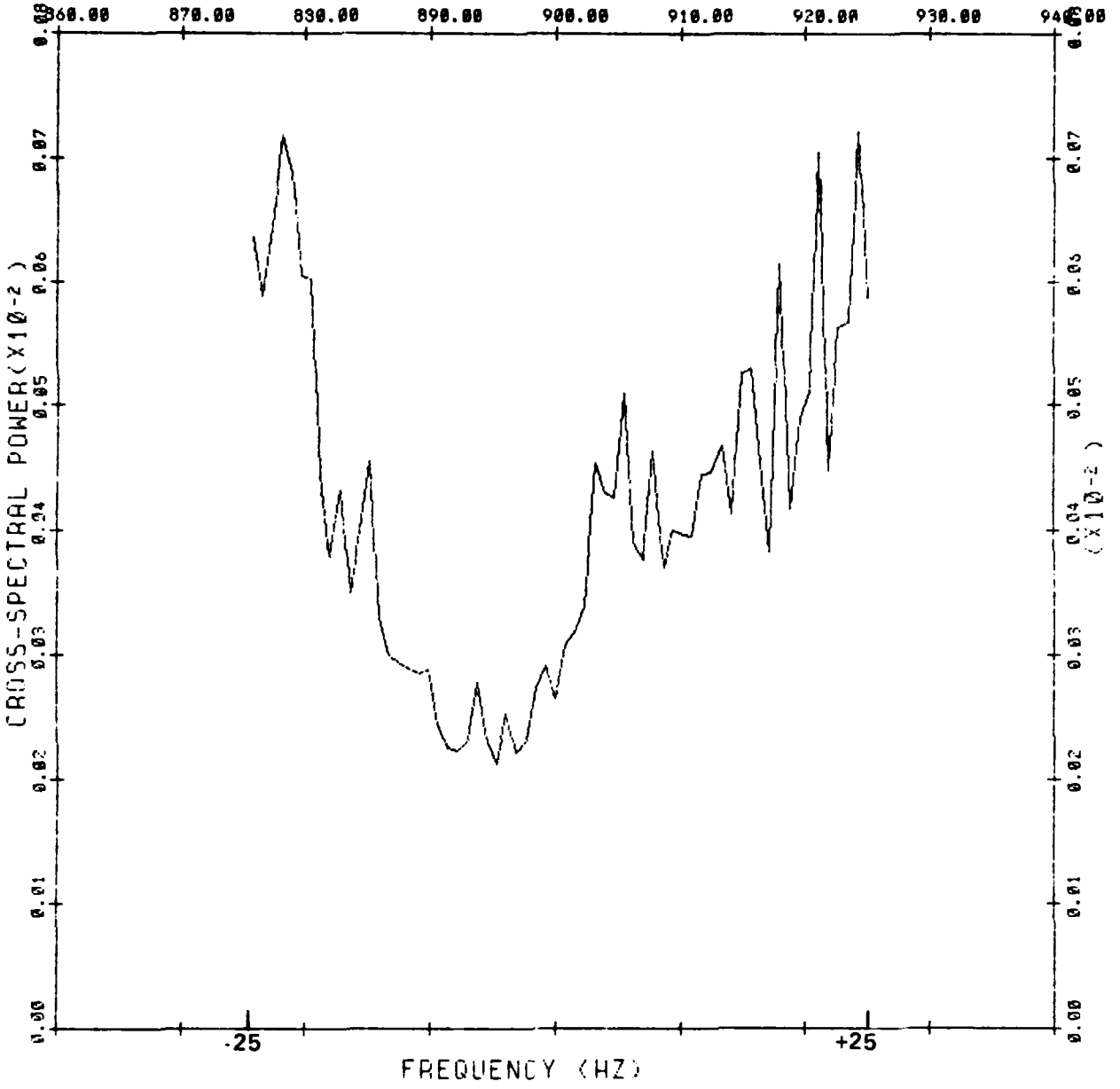

DAY: 27 HOUR: 1 MIN.: 32 SEC.: 0
LAG IN SECONDS FOR CROSS SPECTRUM: 0.00
NUMBER OF SPECTRA AVERAGED: 100
RANGE INDEX: 18

FIGURE 3.5

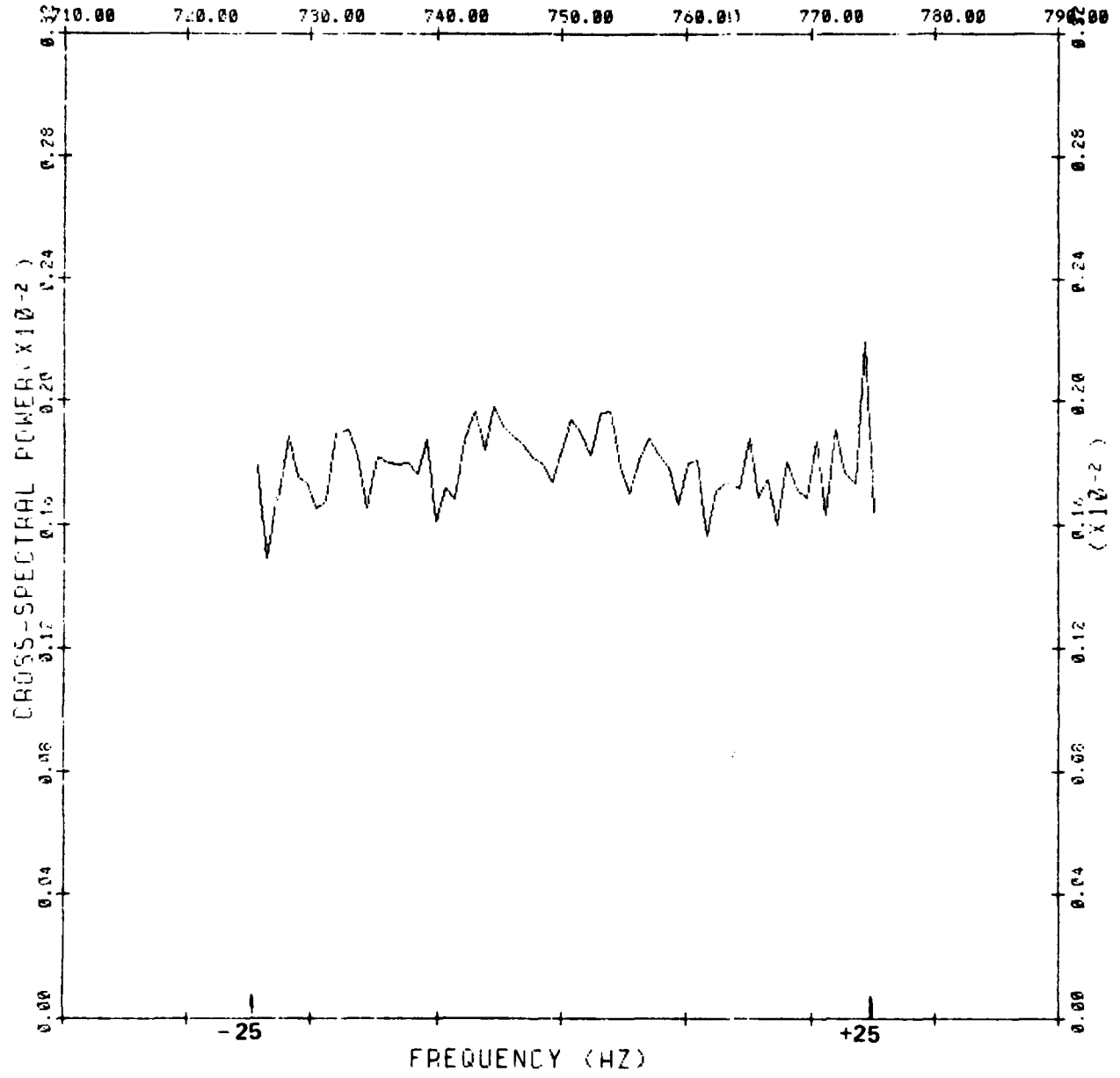

DAY: 27 HOUR: 2 MIN.: 30 SEC.: 0
LAG IN SECONDS FOR CROSS SPECTRUM: 0.00
NUMBER OF SPECTRA AVERAGED: 400
RANGE INDEX: 15

FIGURE 3.6

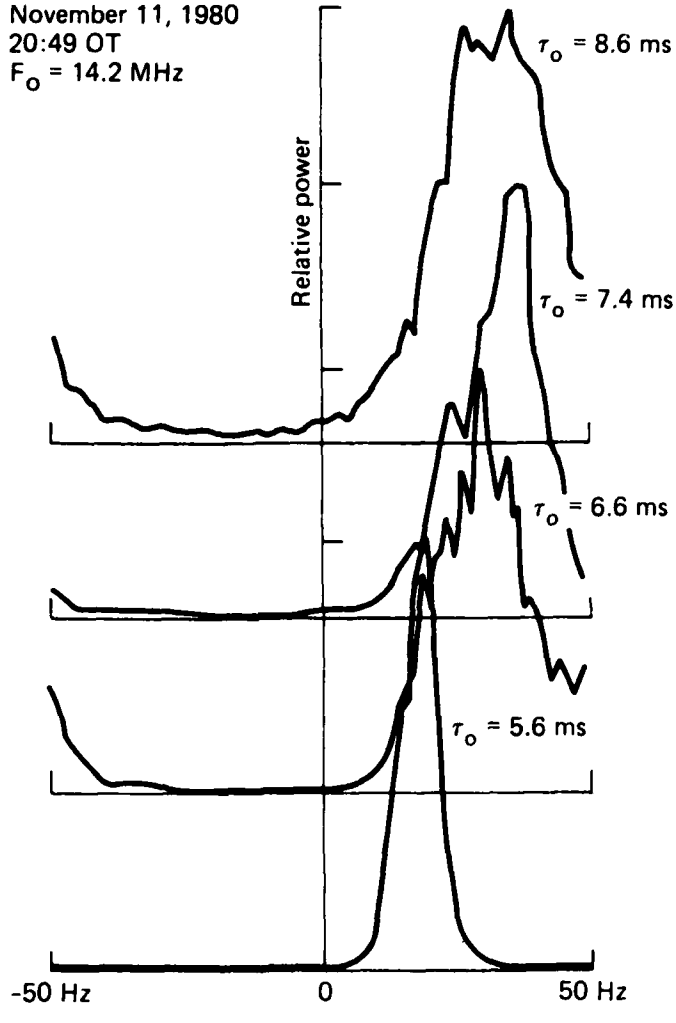
November 11, 1980
20:49 OT
F_o = 14.2 MHz
Relative power
τ_o = 8.6 ms
τ_o = 7.4 ms
τ_o = 6.6 ms
τ_o = 5.6 ms
-50 Hz
0
50 Hz

FIGURE 3.7

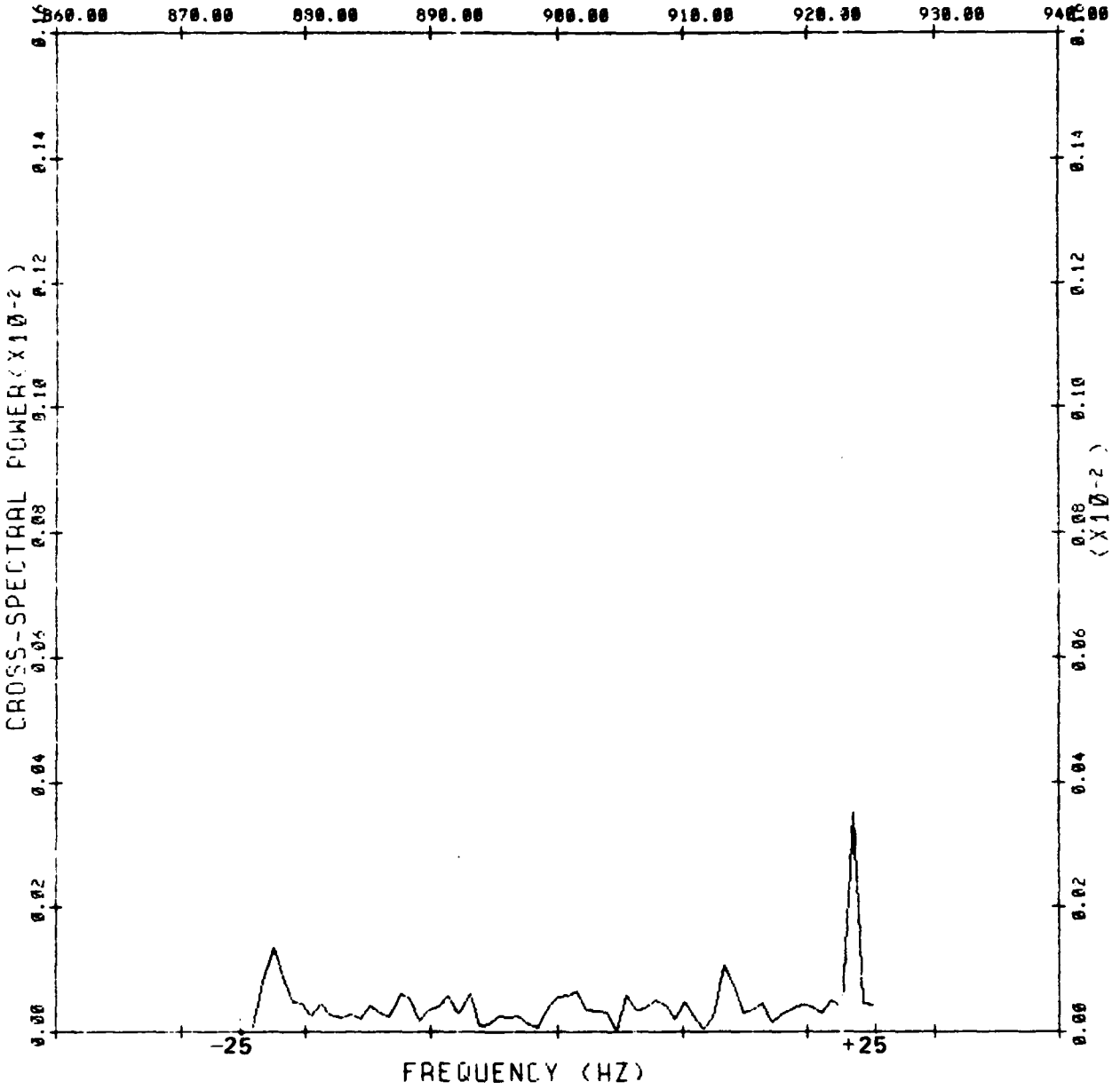

DAY: 27 HOUR: 1 MIN.: 5 SEC.: 30
LAG IN SECONDS FOR CROSS SPECTRUM: 1.28
NUMBER OF SPECTRA AVERAGED: 99
RANGE INDEX: 18

FIGURE 4.1

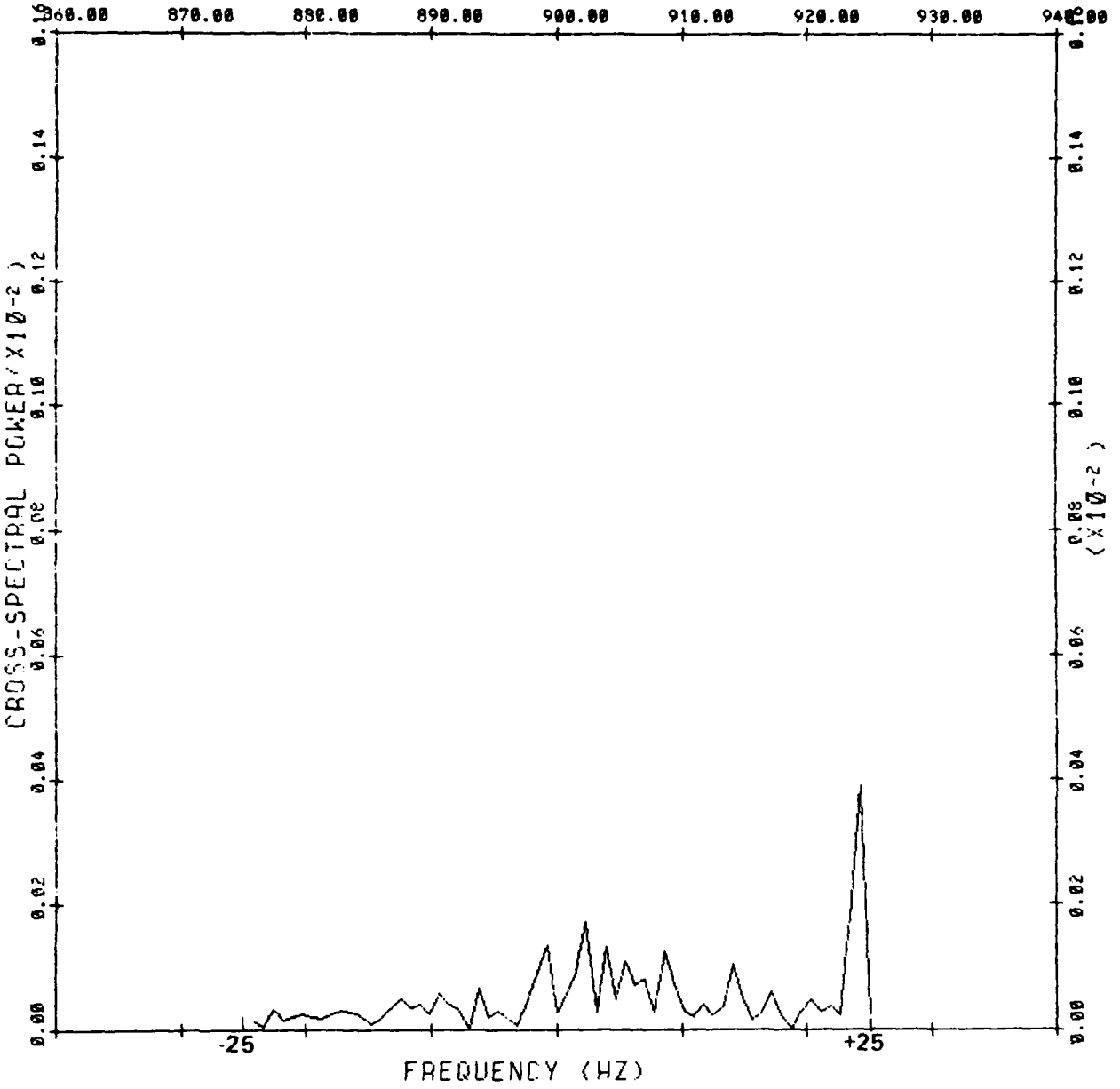

DAY: 27 HOUR: 1 MIN.: 11 SEC.: 0
LAG IN SECONDS FOR CROSS SPECTRUM: 1.28
NUMBER OF SPECTRA AVERAGED: 200
RANGE INDEX: 18

FIGURE 4.2

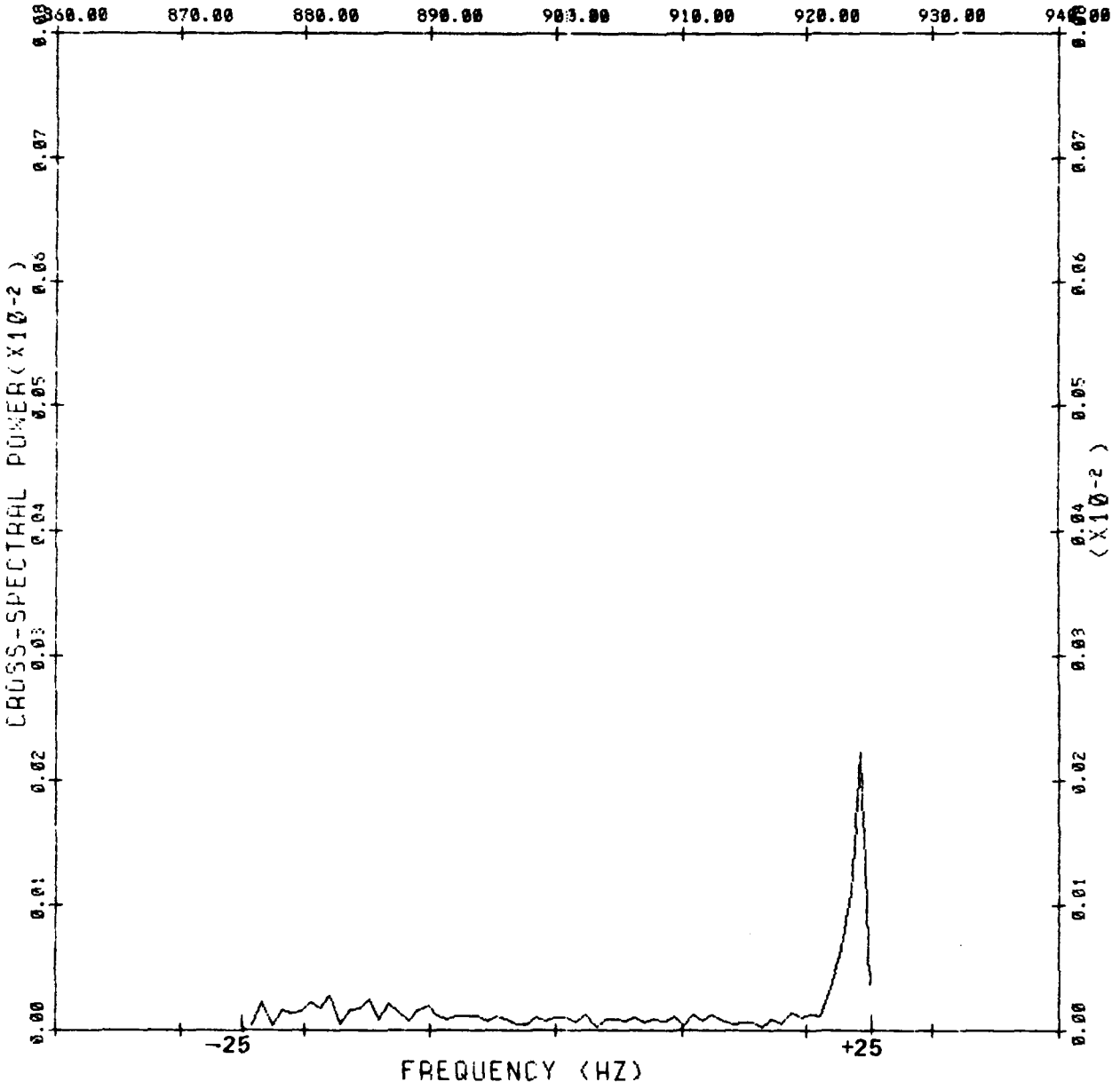

DAY: 27 HOUR: 1 MIN.: 18 SEC.: 0
LAG IN SECONDS FOR CROSS SPECTRUM: 1.28
NUMBER OF SPECTRA AVERAGED: 200
RANGE INDEX: 18

FIGURE 4.3

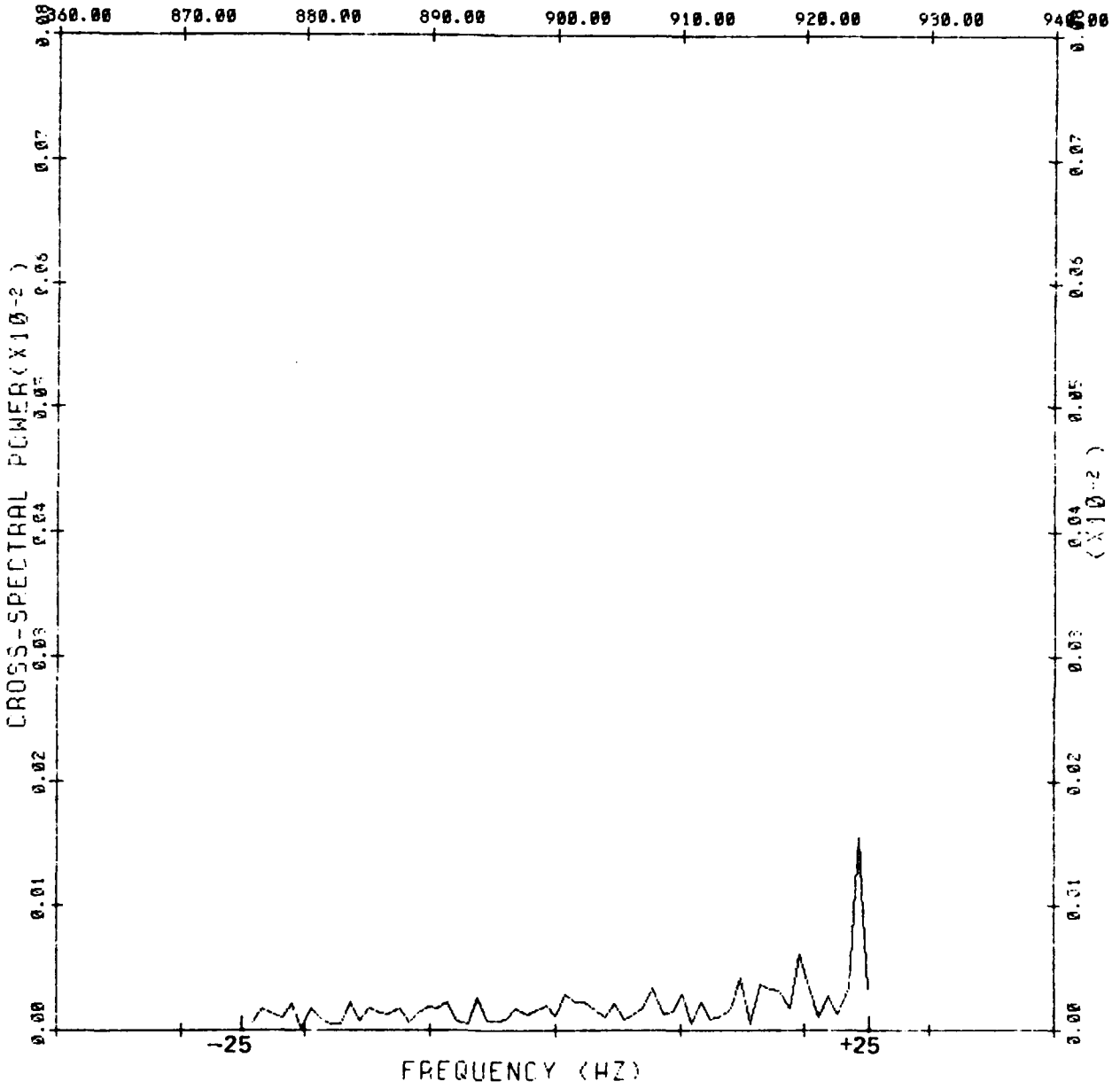

DAY: 27 HOUR: 1 MIN.: 29 SEC.: 0
LAG IN SECONDS FOR CROSS SPECTRUM: 1.28
NUMBER OF SPECTRA AVERAGED: 200
RANGE INDEX: 18

FIGURE 4.4

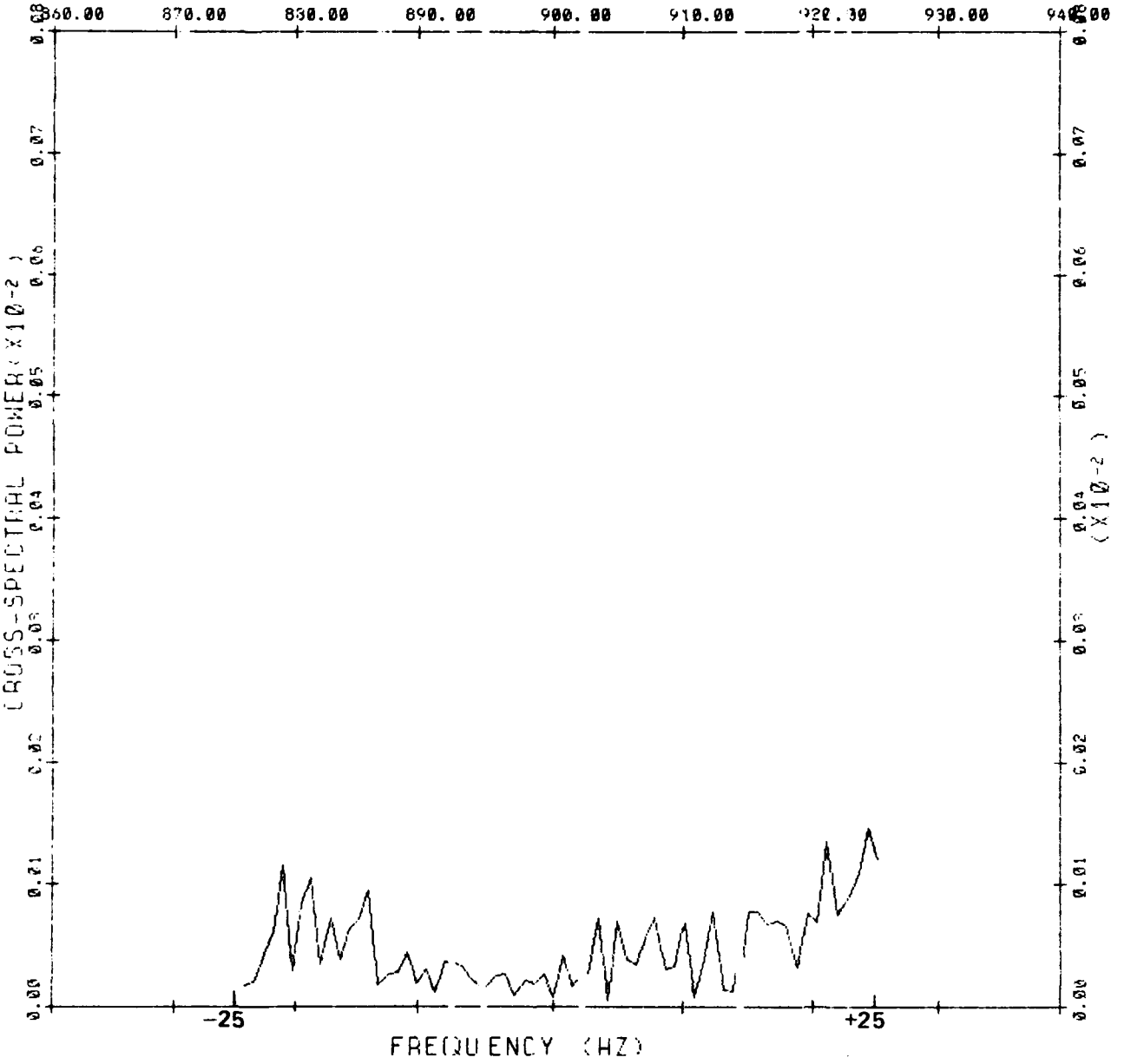

DAY: 27 HOUR: 1 MIN.: 32 SEC.: 0
LAG IN SECONDS FOR CROSS SPECTRUM: 1.28
NUMBER OF SPECTRA AVERAGED: 100
RANGE INDEX: 18

FIGURE 4.5

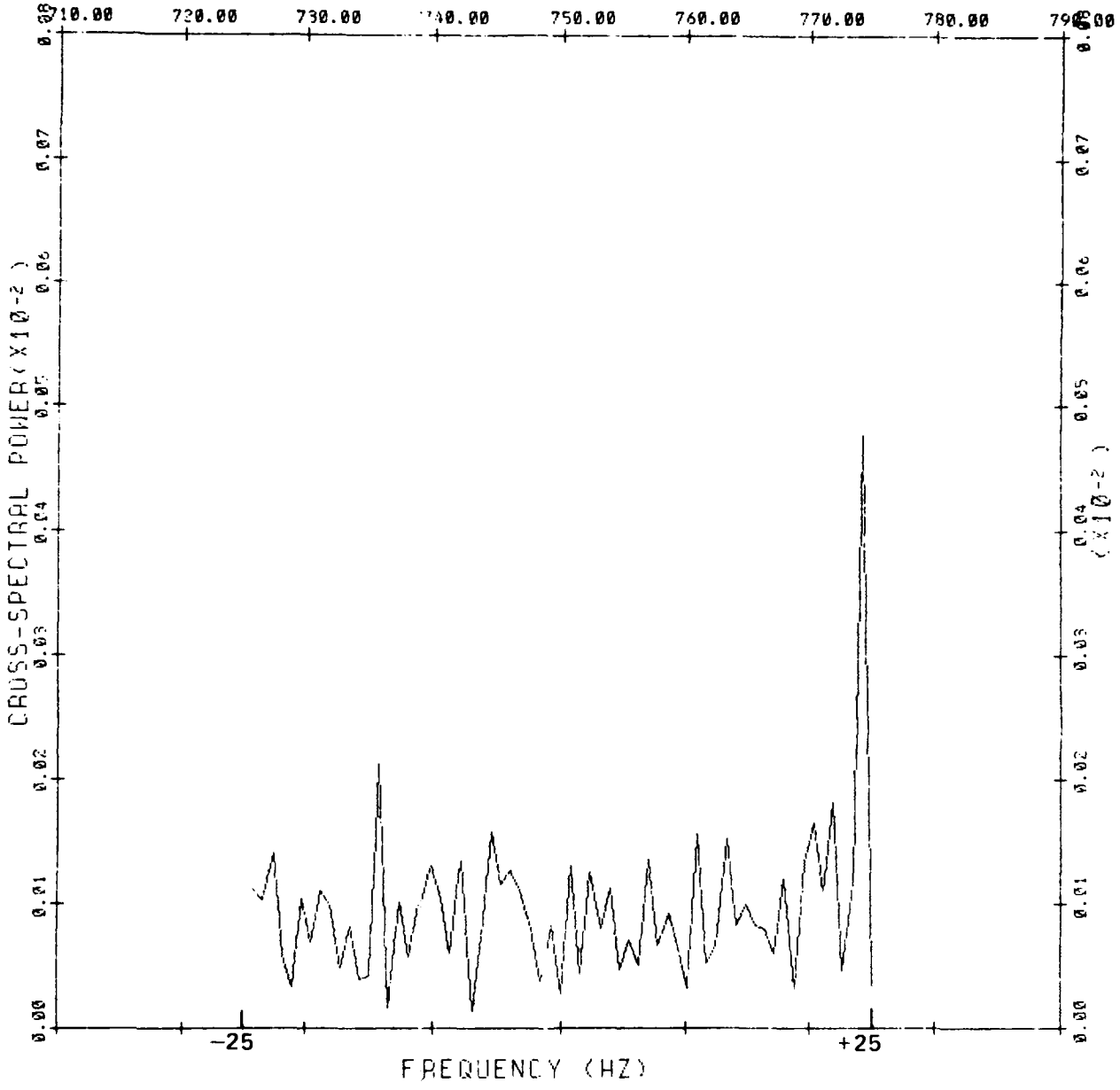

DAY: 27 HOUR: 2 MIN.: 30 SEC.: 0
LAG IN SECONDS FOR CROSS SPECTRUM: 1.28
NUMBER OF SPECTRA AVERAGED: 400
RANGE INDEX: 15

FIGURE 4.6

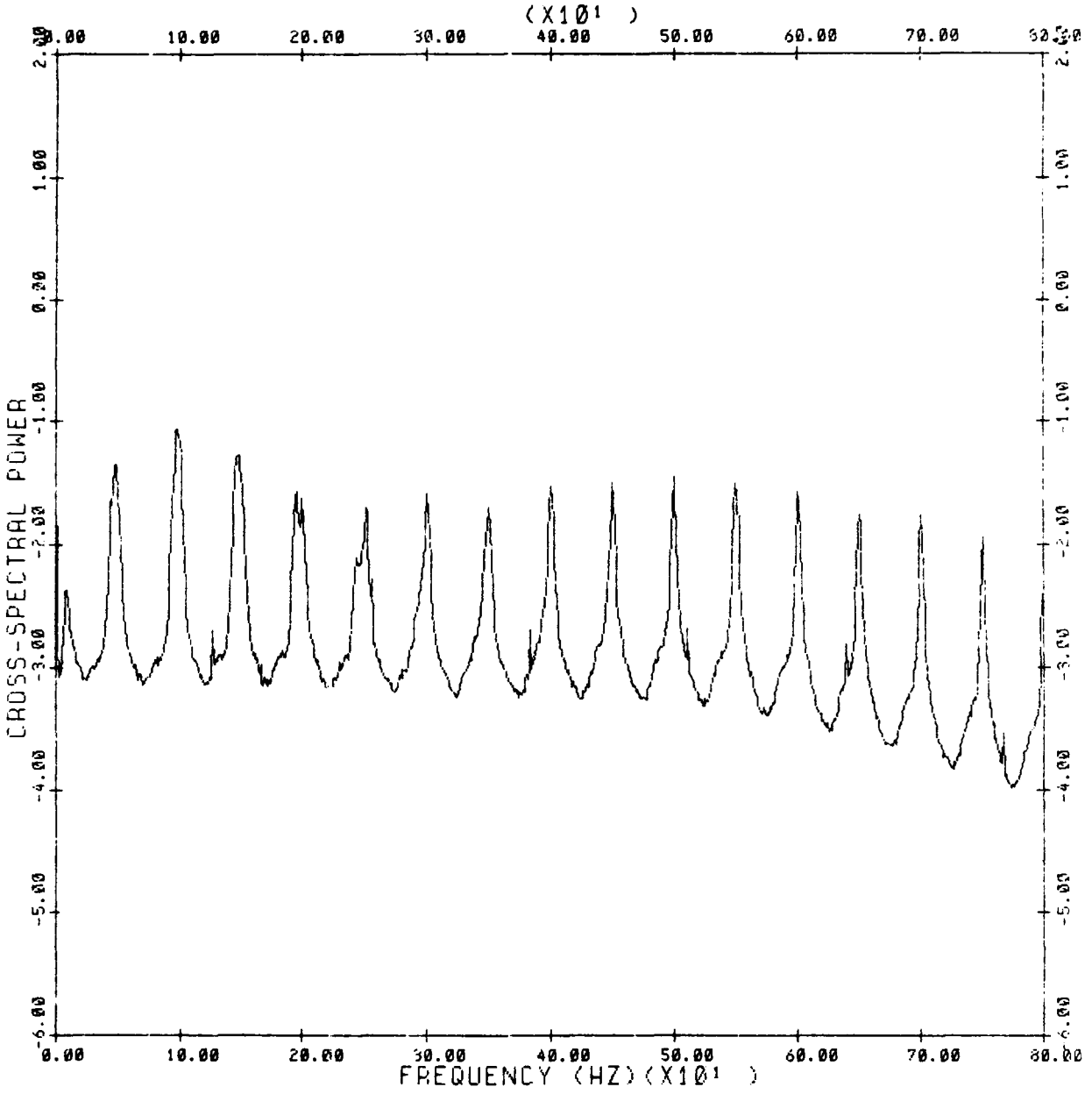

DAY: 346 HOUR: 3 MIN.: 44 SEC.: 0
LAG IN SECONDS FOR CROSS SPECTRUM: 0
NUMBER OF SPECTRA AVERAGED: 999

FIGURE 4.7

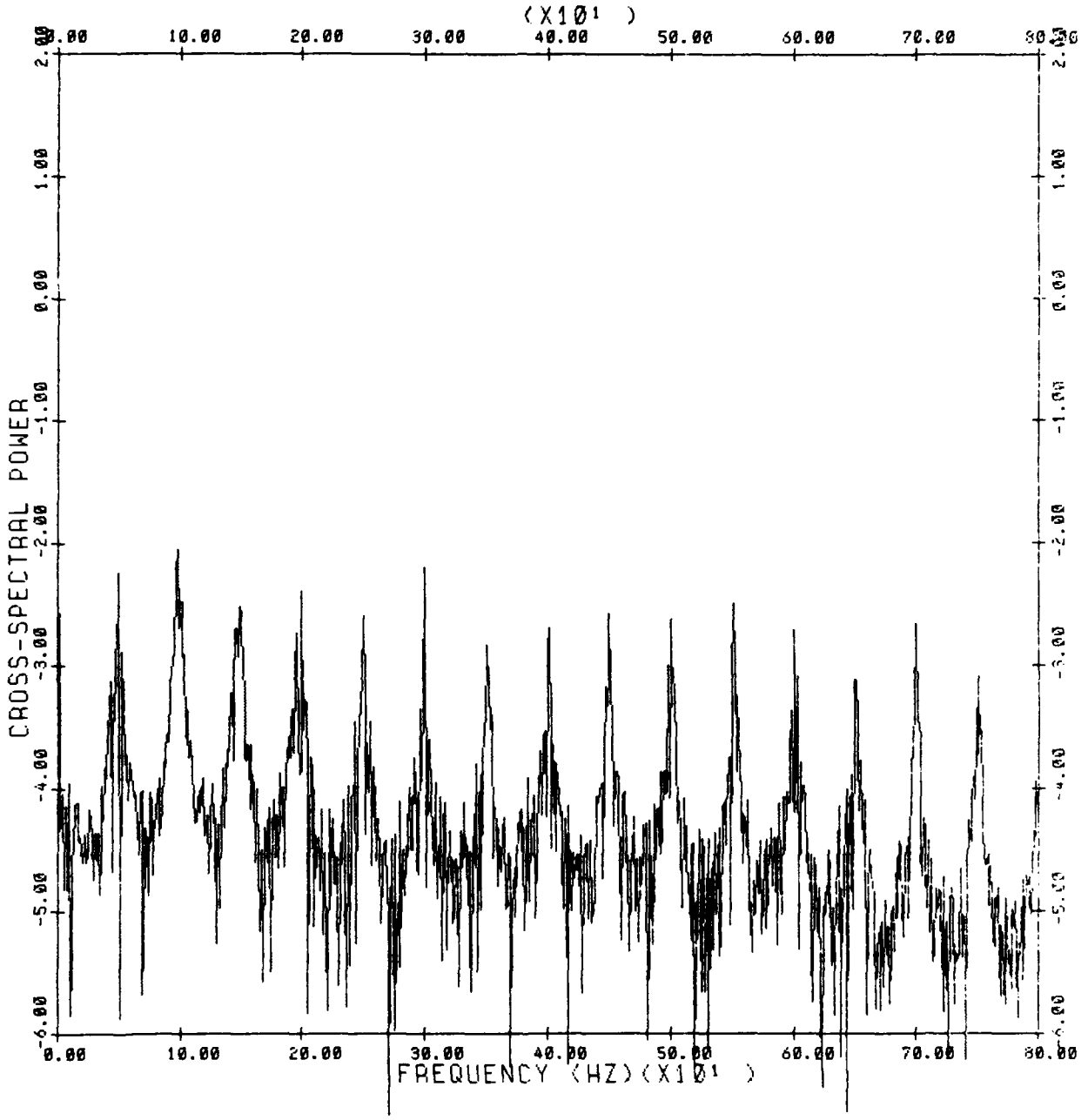

DAY: 346 HOUR: 3 MIN.: 44 SEC.: 0
LAG IN SECONDS FOR CROSS SPECTRUM: 1
NUMBER OF SPECTRA AVERAGED: 999

FIGURE 4.8

MISSION
of
Rome Air Development Center

RADC plans and executes research, development, test and selected acquisition programs in support of Command, Control Communications and Intelligence (C^3I) activities. Technical and engineering support within areas of technical competence is provided to ESD Program Offices (POs) and other ESD elements. The principal technical mission areas are communications, electromagnetic guidance and control, surveillance of ground and aerospace objects, intelligence data collection and handling, information system technology, ionospheric propagation, solid state sciences, microwave physics and electronic reliability, maintainability and compatibility.

Printed by
United States Air Force
Hanscom AFB, Mass. 01731

END

DATE
FILMED

8-82

DTIC